ORIGINAL ARTICLE

Objective characterization of the course of the parasellar internal carotid artery using mathematical tools

Stefan Meng · Stefan H. Geyer · Luciano da F. Costa · Matheus P. Viana · Wolfgang J. Weninger

Abstract

Background Along the internal carotid artery (ICA), atherosclerotic plaques are often located in its cavernous sinus (parasellar) segments (pICA). Studies indicate that the incidence of pre-atherosclerotic lesions is linked with the complexity of the pICA; however, the pICA shape was never objectively characterized. Our study aims at providing objective mathematical characterizations of the pICA shape.

Methods and results Three-dimensional (3D) computer models, reconstructed from contrast enhanced computed tomography (CT) data of 30 randomly selected patients (60 pICAs) were analyzed with modern visualization software and new mathematical algorithms. As objective measures for the pICA shape complexity, we provide calculations of curvature energy, torsion energy, and total complexity of 3D skeletons of the pICA lumen. We further measured the posterior knee of the so-called "carotid siphon" with a virtual goniometer and performed correlations between the objective mathematical calculations and the subjective angle measurements.

Conclusions Firstly, our study provides mathematical characterizations of the pICA shape, which can serve as objective reference data for analyzing connections between pICA shape complexity and vascular diseases. Secondly, we provide an objective method for creating such data. Thirdly, we evaluate the usefulness of subjective goniometric measurements of the angle of the posterior knee of the carotid siphon.

Keywords Blood velocity · Carotid artery · Cardiovascular diseases · Circulation · Three dimensional imaging · Risk factors

S. Meng (✉) · S. H. Geyer · W. J. Weninger
IMG, Center for Anatomy and Cell Biology,
Medical University of Vienna, Waehringer Str. 13,
1090 Vienna, Austria
e-mail: stefan.meng@meduniwien.ac.at

S. Meng
Department of Radiology, Kaiser-Franz-Joseph-Spital,
Kundratstr. 3, 1100 Vienna, Austria

L. da F. Costa · M. P. Viana
Instituto de Física de São Carlos,
Universidade de São Paulo,
Av. Trabalhador São Carlense, 400,
CEP: 13560-970 São Carlos, SP, Brazil

Introduction

The three-dimensional (3D) course of an artery defines the quality and intensity of hemodynamic forces, which affect its wall. Shear stress and wall tension can cause vascular remodeling by triggering gene up-regulation in endothelial cells. Vascular remodeling, in turn can result in vascular pathologies [24]. Especially the twisted segments of the internal carotid artery (ICA) inside the parasellar (cavernous sinus) region—we refer to them as parasellar ICA (pICA)—are frequently affected by vascular diseases [2, 5, 10, 12, 15, 18, 23, 29]. We hypothesize that vascular pathologies of the pICA are directly linked with the complexity of its shape. Therefore, precise definitions of the complexity of the pICA would permit the identification of individuals prone to suffer from pICA lesions and associated neuronal disorders. However, up to now neither a sufficiently objective and thus reliable characterization of the pICA shape, nor methods for performing such a characterization do exist.

Traditionally the pICA is considered as the proximal part of a siphon with an anterior and a posterior knee

[11, 21]. But this view is purely two-dimensional (2D) and neglects the torsion of the blood vessel as well as its transversal bends [7]. More sophisticated descriptions try to take into account the 3D complexity. They comprise a better morphological characterization but do not provide sound quantitative or objective data [1, 6, 13, 14, 16, 17, 22, 25]. The only quantitative data currently available are based on measurements of angles of the two characteristic curves of the so-called carotid siphon in radiographs and dissected specimens [3, 20]; however, due to technical limitations they are subjectively biased and neglect the peculiar 3D component of the pICA curves as well as its torsion.

Our study aims at providing an objective mathematical characterization of the shape of the adult pICA with the aid of new mathematical tools. It further aims at evaluating the significance of subjective goniometric angle measurements for estimating the objective pICA shape complexity.

Material and methods

Contrast media enhanced CT data of 30 randomly selected patients (8 males and 22 females), who were between 22 and 77 years (mean 48.2 years) old, were analyzed in this study. The patients had been scanned with a multislice CT scanner (Somatom Volume Zoom, Siemens, Erlangen, Germany) for a preoperative evaluation of intracranial blood vessels. The examinations were carried out during helical scanning (140 kVp, 100 mAs_{eff}) using a 2×0.5 mm detector configuration and a table feed of 1.2 mm per rotation. Axial sections were reconstructed every 0.3 mm with a section thickness of 0.5–0.75 mm. None of the examined data showing pathologies of the pICA (except for calcifications) or the cavernous sinus region were included. Fifteen patients had normal blood pressure. Ten patients were diagnosed arterial hypertension. The blood pressure documentation of five patients could not be retrieved.

Three-dimensional computer models were generated on a PC using state of the art 3D reconstruction and visualization software (NIH-Image, National Institutes of Health, USA and Amira 4.0, Mercury Systems). The close proximity of the contrast medium enhanced lumen of the ICA with osseous structures hindered the use of automatic contour finding algorithms. Therefore the blood vessels were segmented manually. The proximal end of the pICA was defined by virtual clipping of the 3D data at the level of the internal opening of the carotid canal. Its distal end was defined by virtual clipping of the blood vessel proximal to the origin of the ophthalmic artery (Fig. 1).

We adapted the methodology proposed by Verroust [26] for calculating 3D skeletons (central lines) of the pICAs.
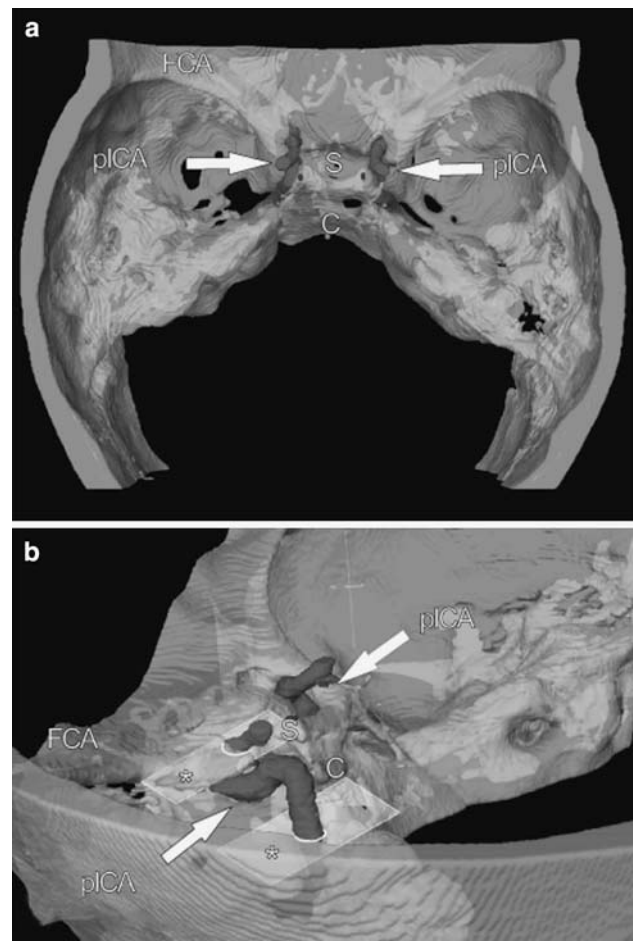

Fig. 1 3D computer models of the left and right pICAs in situ. **a** View from *top*, **b** view from occipitolateral. Note the virtual dissection planes (*asterisk*), which define the pICA (*pICA*). *S*, sella turcica; *C*, clivus; *FCA*, anterior cranial fossa (scale bar 10 mm)

These skeletons were considered as curves in the 3D space. Next, we used differential geometry [9] to estimate the curvature (κ) and torsion (τ) of the arteries. The curvature quantifies the bending of the curve while the torsion measures how much the curve leaves the plane (Fig. 2). These two measurements are local; a value of curvature and a value of torsion are associated to each point along the curve. For example, the curve a in Fig. 2 represents a straight line which has null curvature and null torsion in all points along the curve. In the same figure, the curve b has curvatures different of zero for the points in the red region and null torsion for all its points. In this case, the torsion is null because the whole curve is embedded in the plane. The curve c has non-zero curvature in the plane XY and non-zero torsion in a plane perpendicular to the plane XY, because there the curve moves away from the plane.

After the skeletonization process, the curves were smoothed for eliminating the noise. Special care was invested in retaining the main geometrical aspects of the
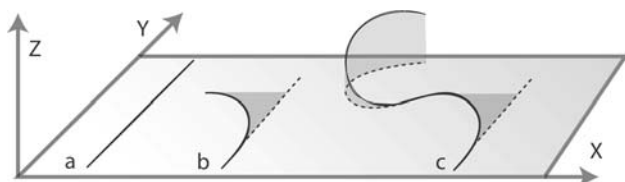
Fig. 2 Defintion of curvature and torsion. Curve *a* has curvature and torsion equal to zero. Curve *b* lies in the plane XY and has non-zero curvature, but zero torsion. Curve *c* leaves the plane XY, and has non-zero curvature and non-zero torsion

arteries. Differential geometry concepts [9] were then used for calculating the curvature and torsion for all points along the skeletons of the arteries. In order to summarize the skeletons geometry into two measurements, we used the concepts of curvature energy (E_κ) and torsion energy (E_τ). Basically, they correspond to the average value of the square curvature and torsion, respectively, over all points of the curve. From these results we evaluate the curvature and torsion energies of the skeletons.

$$E_\kappa = L^2 \frac{1}{N} \sum_{i=1}^{N} k_i^2 \qquad E_\tau = L^2 \frac{1}{N} \sum_{i=1}^{N} \tau_i^2$$

The L^2 factor (L is the total arc length of the skeleton under analysis), which guarantees scale invariance (i.e., any circle will always have the same energy value), is required for comparisons between curves with different lengths. Moreover, it is important to note that both curvature (k_i) and torsion (τ_i) have units inverse of the length (L), implying the energies to be dimensionless. For providing a measure for total complexity, we add the values of curvature and torsion energies. Observe that the 10% of the N points were disregarded at both the curve extremities in order to avoid the respective discontinuities (i.e., the curvature and torsion are not defined at the extremities).

For goniometric angle measurements two 2D screenshot images were captured from each 3D computer model. One screenshot showed a lateral view of the pICA in the perspective view mode of the visualization software. This view of the pICA appears similar to a conventional angiographic image. The second screenshot showed the pICA in the orthogonal mode of the visualization software. This screenshot image was captured after rotating the 3D model into a position, in which a virtual plane through the posterior angle was as close as possible parallel to the screen plane (Fig. 3). In both screenshot images, the angle of the posterior knee of the carotid siphon (PC) was measured with the aid of a virtual goniometer using the Photoshop CS2 software (Adobe System Incorporated).

For statistics, we employed the Student's *t* test and the Pearson's product moment correlation coefficient using the software package SAS (SAS Institute Incorporated).

Results

We present calculations of the curvature and torsion energy and total complexity of the pICA, goniometric measurements of the posterior knee of the carotid siphon, and statistical comparisons between the mathematical shape parameters and the goniometrical measured angles. The results are presented in this sequence.

For the total sample of 60 pICAs, we measured a mean curvature energy of 12.99 (range 0.73–69.13) and a mean torsion energy of 16.71 (range 0.56–131.66). As an indicator for the total complexity of the pICA, we added up curvature and torsion energy. The mean total complexity was 29.70 (range 1.89–163.46). Table 1 informs about details regarding side. Student's *t* test analysis revealed no significant differences in pICA curvature energy ($P = 0.41$), torsion energy ($P = 0.62$), and total complexity ($P = 0.96$) between left and right-sided blood vessels. Statistical analysis also showed a weak to middle correlation of curvature and torsion energy for each blood vessel ($r = 0.368$, $P = 0.0039$). Torsion energy, curvature energy, and total complexity of each patient's left and right pICA (curvature $r = 0.618$, $P = 0.0003$; torsion $r = 0.426$, $P = 0.0188$; total complexity $r = 0.546$, $P = 0.0018$) showed a significant positive correlation.

The 3D computer models of 100% of our specimens showed a well-defined curve in the proximal part of the pICA, the posterior knee of the so-called "carotid siphon" (PC). The apogee of this curve was in all specimens directed upwards. Measurements of its angle in 2D screenshots of the 3D models as displayed in the perspective view modus ranged between 35° and 180° (mean 109°, median 105°). Measurements of the same angle in 2D screenshots of the 3D models as displayed in the orthogonal view modus ranged between 43° and 219° (mean 129°, mode 125.5°). Table 1 informs about details regarding side. The angle measurements obtained from perspective views correlated strongly with the measurements obtained from orthogonal views of the 3D models ($r = 0.899$, $P < 0.0001$) (Fig. 4). Furthermore statistics revealed a strong positive correlation between the dimensions of the PCs of each patient's left and right pICA as measured in perspective views ($r = 0.872$, $P < 0.0001$) and orthogonal views ($r = 0.825$, $P < 0.0001$) (Fig. 5).

For testing whether subjective angle measurements of PC can be used as a measure for estimating the objectively calculated mathematical pICA complexity, we correlated the measures for curvature energy, torsion energy, and total complexity with the degree of PC (Fig. 6). We found a weak positive correlation of PC with torsion energy (perspective projection $r = 0.390$, $P = 0.0020$; orthogonal projection $r = 0.287$, $P = 0.0263$). A stronger correlation was found between PC and curvature energy (perspective

Fig. 3 Goniometric angle measurements; **a** pICA in situ (occipitolateral view). **b** Screenshot of the *left* (*light gray*) and *right* (*dark gray*) pICA in perspective view modus. The measured angle of the proximal pICA curve (*PC*) is drawn in. **c** Screenshot image of the *left* (*light gray*) and *right* (*dark gray*) pICA in orthogonal view modus. Note that the 3D models are rotated and PC of the left pICA is arranged as closely as possible parallel with the screen plane. *C*, clivus; *FCA*, anterior cranial fossa; *f*, frontal; *o*, occipital
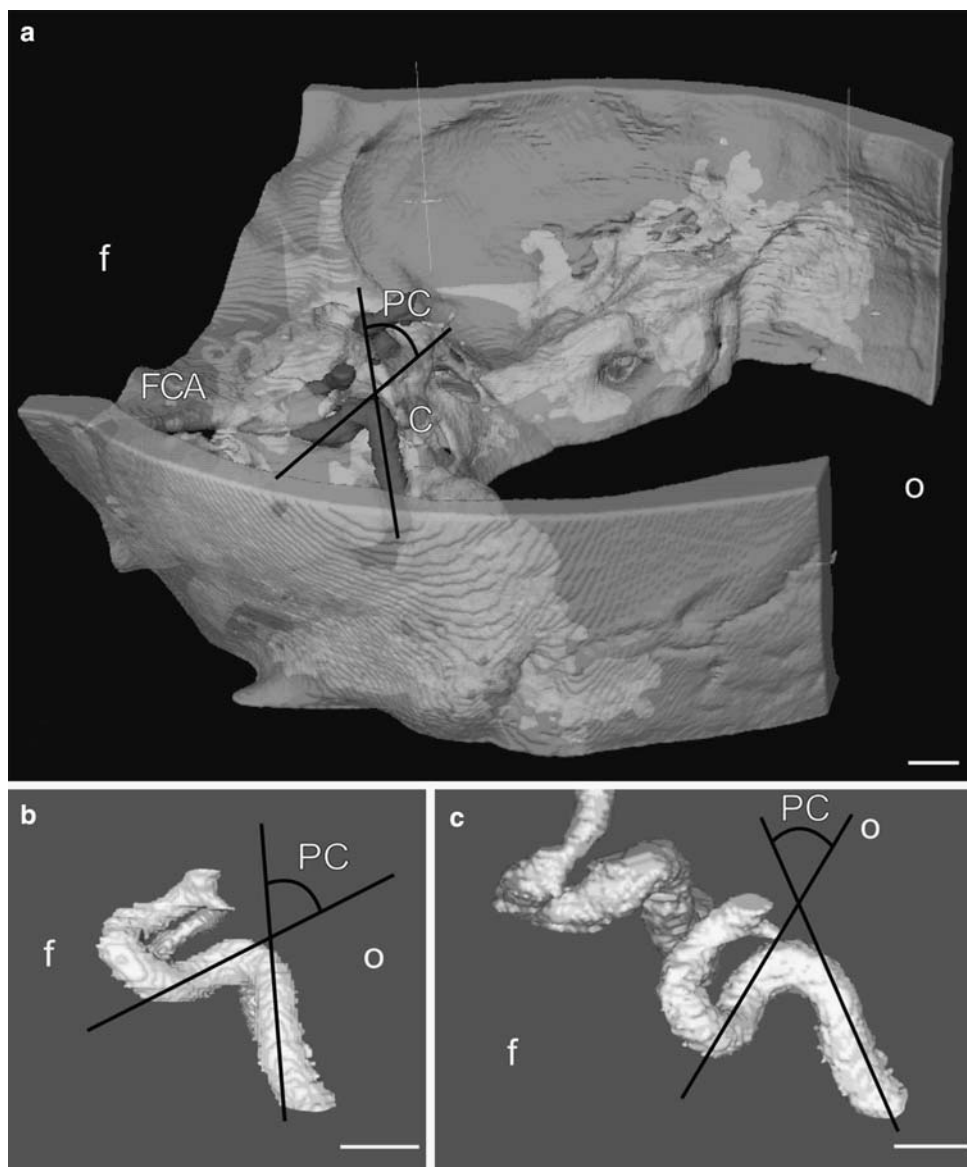

Table 1 Mathematical and goniometric measures for the complexity of the pICA

	cur	tor	total comp	ppm (degrees)	opm (degrees)
Total (*n* = 60)					
Mean	12.99	16.71	29.7	109	129
Range	0.73–69.13	0.56–131.66	1.89–163.46	35–180	43–219
Standard deviation	12.31	17.91	25.19	33	43
Right (*n* = 30)					
Mean	11.66	17.88	29.54	114	134
Range	0.94–43.69	0.56–131.66	1.89–163.46	46–174	43–219
Standard deviation	10.81	23.2	30.28	31	40
Left (*n* = 30)					
Mean	14.32	15.54	29.86	105	125
Range	0.73–69.13	2.09–42.18	2.92–77.50	35–180	61–215
Standard deviation	13.7	10.55	19.33	35	45

cur curvature energy, *tor* torsion energy, *total comp* total complexity energy, *ppm* perspective projection modus, *opm* orthogonal projection modus
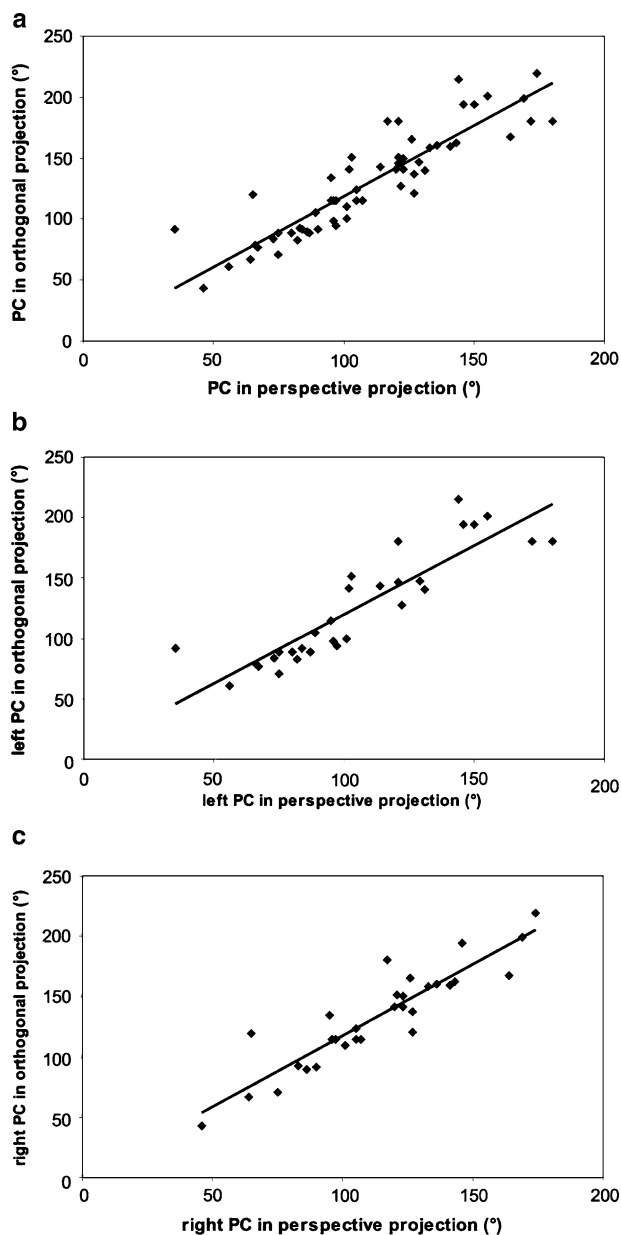
Fig. 4 Correlation between PC dimensions in orthogonal and perspective projection view modus. **a** all pICAs, **b** left pICAs, **c** right pICAs

Fig. 5 Correlation between PC of the *left* and *right* pICAs. **a** Perspective projection view modus and **b** Orthogonal projection view modus

Discussion

High complexity of the shape of a blood vessel usually results from extensive vascular remodeling and is associated with a high risk for suffering from vascular diseases such as atherosclerosis [2, 5, 10, 12, 15, 18, 23, 27]. Pathologies of blood vessels supplying the brain often are responsible for severe cerebral disorders. Especially the parasellar (cavernous sinus) segments of the pICA are heavily bent and twisted. We therefore hypothesize that individuals with a high complexity of the pICA shape have a high risk for developing pICA pathologies and associated cerebral complications. Verification of this hypothesis requires an easy to perform method for generating objective data of shape complexity as well as precise reference data defining the normal shape complexity of the pICA. Our study provides both.

Mathematically the complexity of a blood vessel is defined by the curvature and torsion energy of its 3D skeleton. Previous works have addressed the characterization of the geometrical properties of arteries [8, 19, 30]. The Fourier transform has been suggested as a means to estimate curvature and torsion [4], and Ding and Friedman developed a methodology based on piecewise interpolation by low degree polynomials [8]. Medina et al. [19] compared such approaches and concluded that the Fourier and

projection $r = 0.538$, $P < 0.0001$; orthogonal projection $r = 0.452$, $P = 0.0003$) and between PC and total pICA complexity as defined by the sum of curvature and torsion energy (perspective projection $r = 0.541$, $P < 0.0001$; orthogonal projection $r = 0.425$, $P = 0.0007$).

We compared the group of patients suffering from high blood pressure with the group of patients showing normal blood pressure values. Neither the Wilcoxon rank sum test, nor Students t test revealed significant differences in any of the mathematically calculated or manually measured parameters at $P < 0.05$.
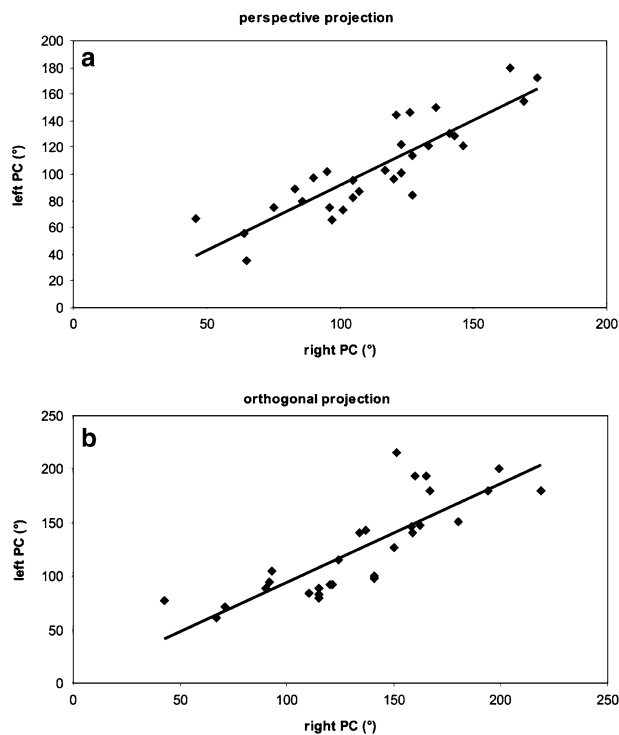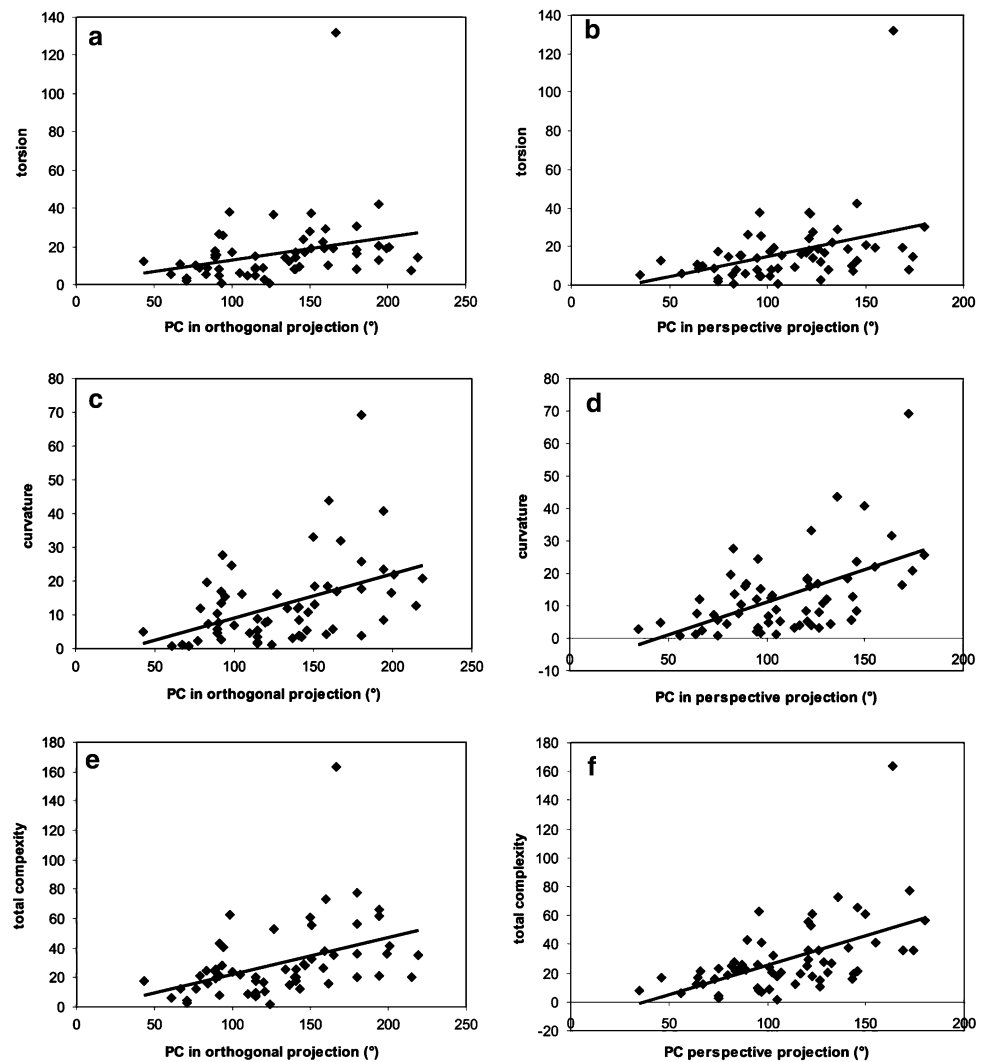
Fig. 6 Correlation between objective mathematical indicators of complexity and subjective angle measurements in orthogonal projection view modus (**a**, **c**, **e**) and perspective projection view modus (**b**, **d**, **f**). **a**, **b** Correlation between torsion energy and PC; **c**, **d** correlation between curvature energy and PC, and **e**, **f** correlation between total complexity and PC

low-degree polynomial approaches tended to be more suited for the estimation of curvature and torsion, respectively. Because the pICAs are relatively smooth, it was possible to fit a single polynomial of degree 9 along the whole curve by using generalized mean squares. Since such a mathematical representation has no discontinuities in any of its derivatives, it was possible to achieve proper estimation of both curvature and torsion.

We used the mathematical tools for providing objective quantitative characterizations of the complexity of the pICA. We provide statistics on curvature energy, torsion energy, and total complexity of the 3D skeletons of the pICAs of 30 randomly selected patients (60 blood vessels) without pathologies of or near the pICA. The 3D skeletons were calculated from 3D computer models derived from contrast enhanced CT data sets. Therefore we are able to present reliable reference data for theoretical and clinical comparative studies, researching connections between pICA shape and vascular pathologies.

The mathematically calculated pICA complexity shows a broad individual variation. The spectrum spans from straight pICAs with almost zero total complexity to heavily twisted pICAs with high values for total complexity. Curvature and torsion energy show only a weak correlation. In contrast to individual variety, all three indicators for objective complexity (curvature energy, torsion energy, and total complexity) show a strong correlation between one patient's left and right pICA. This suggests two consequences. Firstly, the development of the pICA complexity is triggered by the developmental factors, which act bilaterally. Secondly, if shape complexity is associated with vascular pathologies, such pathologies will highly likely occur bilaterally.

Our mathematical definitions are the only reliable basis for objective characterizations of the pICA shape and for reproducible comparisons of its complexity. Due to the lack of adequate methods up to now such characterizations do not exist. The complexity of a blood vessel is usually

defined by measuring the dimension of its angles [3, 20, 28]. We evaluated whether angle measurements of the constant and prominent angle in the proximal part of the pICA (PC)—the so-called posterior knee of the carotid siphon— are of any significance in defining or estimating the complexity of the pICA. We measured PC in both, the orthogonal and perspective display modus of the 3D visualization software. The orthogonal modus eliminates artifacts introduced by perspective distortions and resembles the measurement conditions as found during anatomical dissection. The perspective modus resembles the appearance of the pICA in images obtained with the aid of 2D radiological standard techniques such as routine angiography. Angle measurements obtained in both modalities showed a significant correlation with total complexity and curvature energy of the pICA. Only a weak correlation was seen between the dimension of PC and the torsion energy of the pICA. This demonstrates that simple measurements of posterior knee angles in 2D angiograms and anatomical specimens can provide a rough estimation of the pICA curvature and total complexity. But it also demonstrates that PC is a poor indicator for estimating the torsion energy of the pICA.

Conclusion

We present a method for performing objective mathematical characterizations of the pICA. We used this method for analyzing the pICA shape of adult humans and for creating reference data for researching links between pICA shape complexity and the genesis of vascular pathologies and their consequences, respectively. We further evaluate the usefulness of angle measurements of the posterior knee of the carotid siphon for estimating the objective pICA complexity and discuss the clinical implications of our data.

References

1. Bergland RM, Ray BS, Torack RM (1968) Anatomical variations in the pituitary gland and adjacent structures in 225 human autopsy cases. J Neurosurg 28(2):93–99
2. Borozan PG, Schuler JJ, LaRosa MP, Ware MS, Flanigan DP (1984) The natural history of isolated carotid siphon stenosis. J Vasc Surg 1(6):744–749
3. Chrzanowski R (1971) The assessment of the intracranial part of the internal carotid artery. Neuroradiology 2(4):223–226
4. Costa LdF, Cesar JRM (2001) Shape analysis and classification: theory and practice. CRC Press, Boca Raton
5. Craig DR, Meguro K, Watridge C, Robertson JT, Barnett HJ, Fox AJ (1982) Intracranial internal carotid artery stenosis. Stroke 13(6):825–828
6. Curry RW, Culbreth GC (1951) The normal cerebral angiogram. AJR Am J Roentgenol 65(3):345–373
7. Dei Poli G, Zucha J (1940) Beiträge zur Kenntnis der Anomalien und der Arteria carotis interna. Zentralblatt für Neurochirurgie 5(6):209–238
8. Ding Z, Friedman MH (2000) Dynamics of human coronary arterial motion and its potential role in coronary atherogenesis. J Biomech Eng 122(5):488–492
9. Do Carmo M (1976) Differential geometry of curves and surfaces. Prentice-Hall, Englewood Cliffs
10. Dörfler J (1935) Ein Beitrag zur Frage der Lokalisation der Arteriosklerose der Gehirngefäße mit besonderer Berücksichtigung der arteria carotis interna. Arch Psychiatr 103:180–190
11. Fischer E (1938) Die Lageabweichung der vorderen Hirnarterie im Gefäßbild. Zentralblatt für Neurochirurgie 5(3):300–317
12. Fisher CM, Gore I, Okabe N, White PD (1965) Calcification of the carotid siphon. Circulation 32(4):538–548
13. Hasso AN, Bentson JR, Wilson GH, Vignaud J (1975) Neuroradiology of the sphenoidal region. Radiology 114(3):619–627
14. Jovanovic S (1971) [Variations and development of the internal carotid artery curves in the cavernous sinus]. Glas Srp Akad Nauka [Med] 23:163–173
15. Kappelle LJ, Eliasziw M, Fox AJ, Sharpe BL, Barnett HJ (1999) Importance of intracranial atherosclerotic disease in patients with symptomatic stenosis of the internal carotid artery. The North American symptomatic carotid endarterectomy trail. Stroke 30(2):282–286
16. Knosp E, Muller G, Perneczky A (1988) The paraclinoid carotid artery: anatomical aspects of a microneurosurgical approach. Neurosurgery 22(5):896–901
17. Kozlowski P (1963) Relation of the internal carotid siphon to the carotid sulcus. Acta Radiol Ther Phys Biol 1:328–331
18. Marzewski DJ, Furlan AJ, St Louis P, Little JR, Modic MT, Williams G (1982) Intracranial internal carotid artery stenosis: long-term prognosis. Stroke 13(6):821–824
19. Medina R, Wahle A, Om E, Sonka M (2004) Curvature and torsion estimation for coronary-artery motion analysis. Proc SPIE 5369:504–515
20. Michailow SS (1964) Makro-und mikroskopische Untersuchungen des Baues des Sinus cavernosus. Anat Anz 115:233–255
21. Moniz E (1940) Die cerebrale Arteriographie und Phlebographie. In: Bumke O, Foerster O (eds) Handbuch der Neurologie. Springer, Berlin
22. Platzer W (1957) Die Variabilität der Arteria carotis interna im Sinus cavernosus in Beziehung zur Variabilität der Schädelbasis. Gegenbaurs Morphologisches Jahrbuch 98:227–243
23. Raju S, Fredericks RK (1987) Carotid siphon stenosis. J Cardiovasc Surg (Torino) 28(6):671–677
24. Resnick N, Yahav H, Shay-Salit A, Shushy M, Schubert S, Zilberman LC, Wofovitz E (2003) Fluid shear stress and the vascular endothelium: for better and for worse. Prog Biophys Mol Biol 81(3):177–199
25. Schiefer W, Vetter K (1957) Das zerebrale Angiogramm in den verschiedenen Altersstufen. Zentralblatt für Neurochirurgie 17(4):218–231
26. Verroust A, Lazarus F (2000) Extracting skeletal curves from 3D scattered data. The Visual Computer 16:15–25
27. Wechsler LR, Kistler JP, Davis KR, Kaminski MJ (1986) The prognosis of carotid siphon stenosis. Stroke 17(4):714–718
28. Weninger WJ, Müller GB (1999) The parasellar region of human infants: cavernous sinus topography and surgical approaches. J Neurosurg 90(3):484–490

29. Weninger WJ, Müller GB, Reiter C, Meng S, Rabl SU (1999) Intimal hyperplasia of the infant parasellar carotid artery: a potential developmental factor in atherosclerosis and SIDS. Circ Res 85(10):970–975

30. Zhu H, Friedman MH (2003) Relationship between the dynamic geometry and wall thickness of a human coronary artery. Arterioscler Thromb Vasc Biol 23(12):2260–2265